Simulation of Correlated Non-Gaussian Pressure Fields

K. GURLEY[1] and A. KAREEM[2]

[1]*University of Florida, Department of Civil Engineering; Gainesville, FL, 32611, USA*
[2]*University of Notre Dame, Department of Civil Engineering and Geological Sciences; Notre Dame, IN, 46556, USA*

Abstract. Among a host of techniques developed for the analysis and prediction of nonlinear structural response, simulation methods are gaining popularity as computational efficiency increases. Implementation of time domain methods require simulated load time histories with case-specific statistical and spectral characteristics. When the assumption of Gaussian wind loading is inappropriate, techniques for simulating non-Gaussian loading must be sought. Over a larger expanse of building surface, simulation of correlated loads at several spatially separated locations is required. This work introduces a multi-variate non-Gaussian simulation method capable of producing realizations with a wide range of spectral and probabilistic characteristics. The correlation between multiple locations is accurately simulated simultaneously, while retaining the appropriate spectral and probabilistic content at each location.

Sommario. Tra la varie tecniche per l'analisi e la previsione della risposta structurale non lineare, stanno acquistando grande popolarità i metodi di simulazione poiché incrementano l'efficienza computazionale. L'implementazione dei metodi nel domino del tempo richiede la simulazione di storie temporali di carico con specifiche caratteristiche statistiche e spettrali. Quando l'ipotesi di gaussianità dell'azione del vento non risulta adeguata può essere necessario ricorrere a techniche di simulazione di carichi non gaussiani. Per superfici di edifici più estese è richiesta la simulazione di carichi correlati in diverse posizioni separate spazialmente. La presente memoria introduce un metodo di simulazione multivariata non-gaussiana capace di riprodurre realizzazioni con un ampio campo di caratteristiche spettrali e probabilistiche. La correlazione tra le molteplici posizioni viene simulata simultaneamente in modo accurato mantenendo in ciascuna posizione caratteristiche spettrali e probabilistiche appropriate.

1. Introduction

The assurance of the safety of structural envelopes subjected to wind loads requires the consideration of non-Gaussian pressure fluctuations. Many of the studies encompassing analysis and modeling of wind effects on structures have tacitly assumed that the involved random processes are Gaussian. This assumption has been invoked primarily for the convenience in analysis, since information concerning statistics of Gaussian processes is abundant. This assumption is valid for integral load effects of the random pressure field.

Regions of structures under separated flows experience strong non-Gaussian effects in the pressure distribution characterized by high skewness and kurtosis. These non-Gaussian loads may be highly correlated over the characteristic dimensions of the entire separation region, eliminating the applicability of the central limit theorem. The non-Gaussian effects in pressure result in non-Gaussian local loads, and give way to increased expected damage in glass panels and higher fatigue effects on other components of cladding. The thrust of the work reported here is the

development of new methods of simulating correlated random processes at spatially separated locations, focusing on the simulation of typical non-Gaussian wind pressure fluctuations under separated flow regions. The technique is introduced first with respect to a single location, then extended to multiple locations. Several examples demonstrate the applicability of the method.

The simulation of Gaussian processes has been explored for several decades, while non-Gaussian simulation has not been as widely addressed. Recent efforts have concentrated on a variety of iterative and non-iterative adaptive correlation-based spectral and ARMA methods [1, 7, 14]. This idea has also been extended to non-Gaussian conditional simulation techniques [2]. A sample of several available time series methods can be found in [5], including filtered Poisson processes [9], ARMA models driven by non-Gaussian noise [8], and alpha stable processes. This work focuses on a robust new method that is appropriate for a wide number of applications, including classes not included in the above samplings.

2.   Modified Hermite Polynomial Static Transformation

An earlier study [7] presents the development of the so-called forward and backward Modified Hermite Transformations. Forward transformation produces a non-Gaussian process, x, through static transformation of a Gaussian process, u, through [12]

$$x = u + h_3(u^2 - 1) + h_4(u^3 - 3u). \tag{1}$$

The forward Modified Hermite Transform identifies the optimum values for the polynomial coefficients h_3 and h_4 such that x precisely matches the desired values of skewness and kurtosis. The backward Modified Hermite Transform identifies the appropriate coefficients in the inverse of equation (1) to produce a Gaussian process, u, from a non-Gaussian process, x. A standard optimization routine is used to identify the most appropriate coefficients constrained by the desired higher order statistics.

The forward and backward Modified Hermite Transformations are applied in a robust non-Gaussian simulation algorithm in the next section.

3.   Spectral Correction: A Non-Gaussian Simulation Technique

Spectral correction is a robust new non-Gaussian simulation method which utilizes user specified non-Gaussian characteristics and frequency content in the form of target moments through fourth order and a target power spectrum. Alternatively, the user may define non-Gaussian characteristics through a numerical PDF model.

A schematic of the method is shown in Figure 1, and consists of a moment correction and spectral correction transformations in series. An iterative application of both corrections provides convergence to the desired spectral and probabilistic characteristics.

Following from the top left in the schematic, the target spectrum G^T is applied to produce a Gaussian process u using a standard Gaussian simulation routine [e.g. 4, 11]. u is sent through a moment correction transformation, consisting of a forward Modified Hermite transformation to yield a process x which matches the desired skewness and kurtosis ($u \rightarrow x$). This non-Gaussian process x has a power spectrum G^x which no longer matches the target spectrum G^T due to distortions in the transformation. The process x is sent through a spectral correction to produce x_c which fits the target spectrum G^T, and maintains the phase in $x(x \rightarrow x_c)$. The spectral
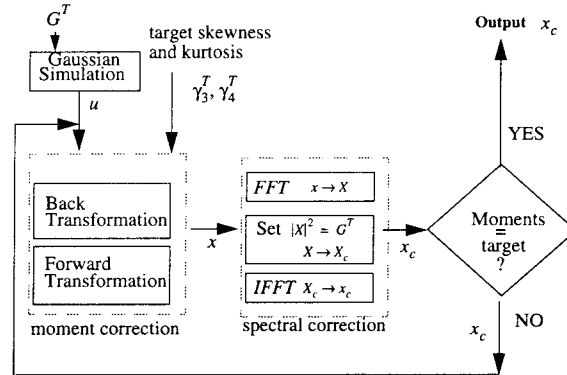
Figure 1. Schematic of the spectral correction non-Gaussian simulation method.

correction transformation from x to x_c distorts the skewness and kurtosis corrected in x. The skewness and kurtosis of x_c are compared with the target values using

$$\mathrm{err} = \left| \frac{\gamma_3^T - \gamma_3}{\gamma_3^T} \right| + \left| \frac{\gamma_4^T - \gamma_4}{\gamma_4^T} \right|, \tag{2}$$

where γ_3^T, γ_4^T are the target skewness and kurtosis, and γ_3, γ_4 are the measured skewness and kurtosis from x_c.

If the error, err, is unacceptably large, the second iteration begins by sending the process with the correct spectrum and distorted skewness and kurtosis, x_c, back to the top of the loop to the moment correction. Here the skewness and kurtosis are again corrected using the backward and then forward Modified Hermite Transform to produce the second iteration of $x(x_c \rightarrow x_2)$.

The iterations continue, checking the error, err, after each spectral correction transform, until the distorted moments of x_c converge to the target moments within a set tolerance. The spectrum of the resulting simulated process matches the target, and the skewness and kurtosis will be within user specified tolerance. Typically two or three iterations are required for convergence [6].

The Modified Hermite Transform in the moment correction section of the iteration may be replaced with a CDF-type mapping transformation when the PDF model associated with the modified Hermite transform is inappropriate [3]. This gives the user the option of describing the non-Gaussian characteristics of the desired process with either the first four moments, or a PDF model.

Example: Simulated Non-Gaussian Suction Pressure on a Rooftop

This example uses full scale pressure data measured simultaneously at several locations on the roof of an instrumented building at Texas Tech University. The Spectral Correction algorithm is used to simulate measured samples of pressure data in a separated flow region.

The left side of Figure 2 shows a comparison of the measured data sample and a single simulation realization. The realization is generated using a target spectrum estimated from the data and the first four measured moments as input. Note the similar characteristics including strong negative skewness, dominant low frequency content, and frequent clustered extreme peaks. These similarities are better seen through comparisons of the power spectral density and probability density function estimated from the measured data and simulated data in the right side of Figure 2. The Spectral Correction simulation method closely emulates these important characteristics in the measured non-Gaussian data. In fact these comparisons can be improved

further by simply reducing the allowable error tolerance in the spectral correction algorithm, at the cost of an additional iteration or two.

4. Multi-Variate Spectral Correction

Spectral correction is extended to include multi-variate simulation, where more than one non-Gaussian correlated time history are generated simultaneously. Multi-variate simulation becomes necessary for cases where non-Gaussian processes at spatially distributed locations are desired. For example, simulation of pressure distributed along the roof of a building, where large scale turbulent flow is correlated across the entire structure.

The univariate algorithm in the previous section begins with a single Gaussian simulation, and iteratively corrects the power spectrum and PDF of the simulated realization. The multi-variate spectral correction simulation algorithm starts with a multi-variate Gaussian simulation, applies iterative corrections to the power spectrum and PDF of each process, and additionally to the cross-spectrum used to simulate the initial Gaussian processes. The iterative corrections to the cross-spectrum result in a convergence to the desired correlation between the resulting simulated non-Gaussian processes.

In order to facilitate this correlation correction, the updating scheme operates on the time domain equivalent of the cross-spectrum, the cross correlation function, given in terms of the cross-spectrum by

$$R_{ij}^T(\tau) = \int_{-\infty}^{\infty} S_{ij}^T(f)\, e^{\sqrt{-1}(2\pi f)\tau}\, \mathrm{d}f, \tag{3}$$

where $S_{ij}^T(f)$ is the two sided target cross-spectral density function between the ith and jth processes. A pair of simulated processes with the same cross-correlation function as the target, $R_{ij}^{x_{\mathrm{NG}}}(\tau) = R_{ij}^T(\tau)$, will properly reflect the desired correlation between the ith and jth processes.

A schematic representation of the multi-variate simulation algorithm is given in Figure 3. Beginning at the top right, the target auto-spectrum, G_{ij}^T, and target skewness and kurtosis, γ_3^T, γ_4^T, of each process is input to the algorithm, along with the target cross correlation function between each pair of processes, R_{ij}^T. A standard multi-variate Gaussian simulation method [e.g. 10, 13] produces a set of Gaussian processes with the design cross-correlation function, R_{ij}^D, and target auto-spectrum, G_{ii}^T. This design cross-correlation is initially set to the target cross-correlation function for the first iteration ($R_{ij}^D(it = 1) = R_{ij}^T$). Each of the Gaussian processes is then transformed to non-Gaussian with its assigned power spectrum and PDF using univariate spectral correction ($x_{\mathrm{G}}^i \rightarrow x_{\mathrm{NG}}^i$). The cross-correlation between these non-Gaussian processes are measured, $R_{ij}^{x_{\mathrm{NG}}}$, and compared with the target values, R_{ij}^T. If the error is too large, a second iteration is begun, otherwise the set of processes x_{NG}^i are accepted as the output.

Before the algorithm begins a new iteration, the design cross-correlation used to generate the Gaussian processes is updated using

$$R_{ij}^D(it + 1) = \left(\rho_{ij}^D(it) + \frac{|\rho_{ij}^D(it)|[\rho_{ij}^T - \rho_{ij}^{x_{\mathrm{NG}}}(it)]}{\max(|\rho_{ij}^D(it)|)} \right) (\max(|R_{ij}^T|)) \tag{4}$$
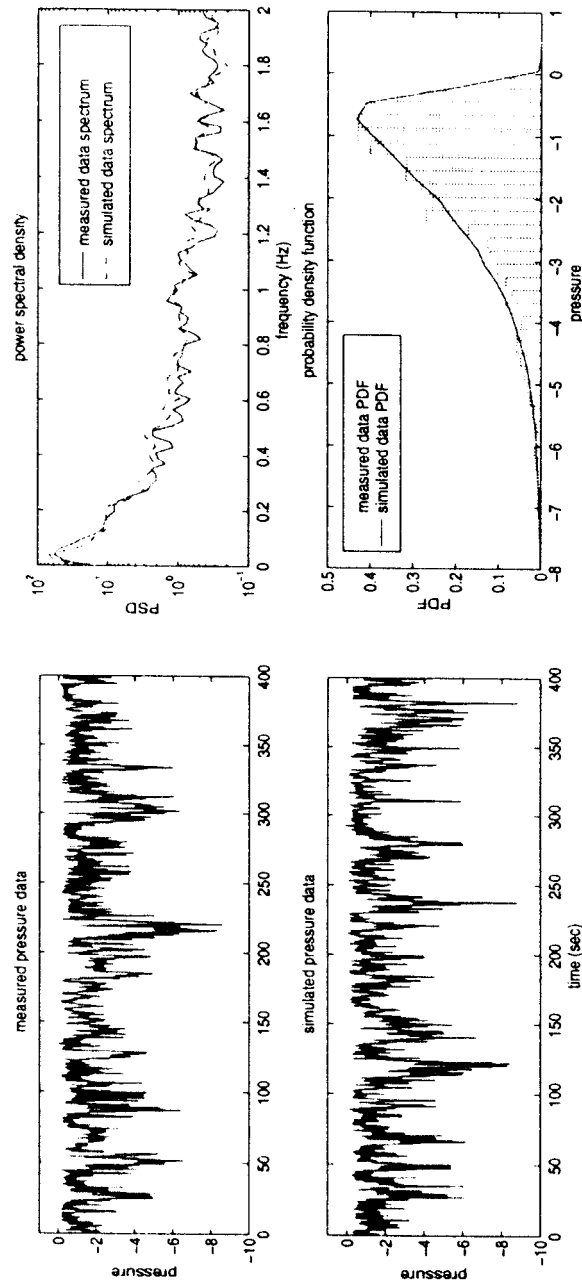
Figure 2. Left: Measured and simulated pressure data. Right: Power spectral density and probability density function of measured and simulated pressure data.
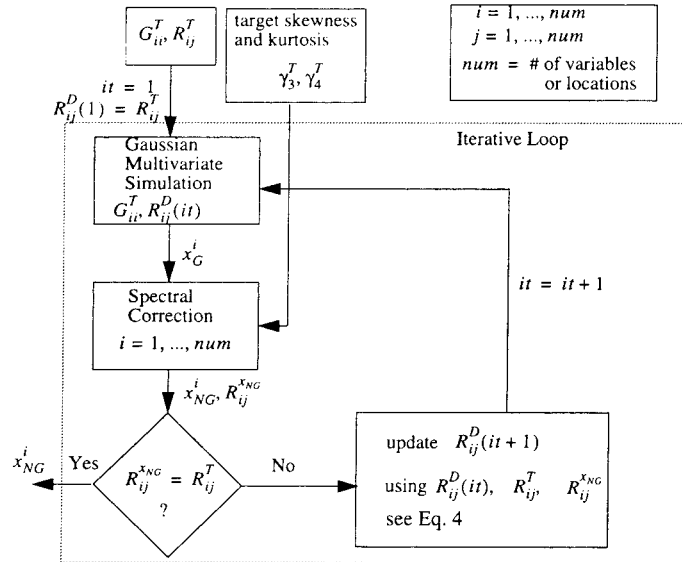
Figure 3. Schematic of the Multivariate Spectral Correction Simulation method.
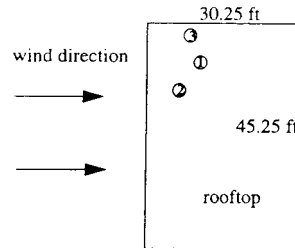

Figure 4. Location of pressure taps on Texas Tech building.

where

$$\rho_{ij}^D(\tau) = \frac{(R_{ij}^D(\tau))}{(\max(|R_{ij}^T(\tau)|))}, \qquad \rho_{ij}^T(\tau) = \frac{(R_{ij}^D(\tau))}{(\max(|R_{ij}^T(\tau)|))},$$

$$\rho_{ij}^{x_{NG}}(\tau) = \frac{(R_{ij}^{x_{NG}}(\tau))}{(\max(|R_{ij}^T(\tau)|))}. \tag{5}$$

Typically two or three iterations provides convergence to the target cross-correlation function between the processes.

Example: Rooftop Pressure at Three Locations

This example again uses the full scale pressure data, measured simultaneously at several locations on the roof of an instrumented building at Texas Tech University. We consider three locations on the roof in a separation zone where the pressure is highly non-Gaussian. The goal of this example is to generate realizations of three pressure records which maintain the cross-spectral density between the measured records, while properly reflecting the higher order statistics and spectral contents at each of the three locations.
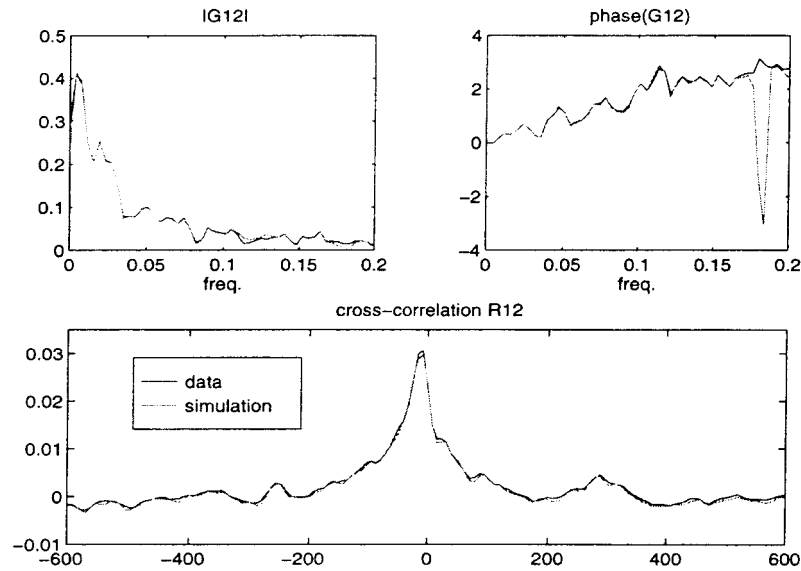
Figure 5. Comparisons of measured and simulated correlation statistics. Top left: Absolute value of the cross-spectrum between locations 1 and 2, Top right: phase of the cross-spectrum between locations 1 and 2 Bottom: cross-correlation function.

Figure 4 is a diagram of the approximate locations of the pressure taps, slightly offset from each other both parallel and perpendicular to the incoming wind. This offset leads to a non-zero phase relationship between locations, as the turbulent wind field arrives at each location at slightly different times.

Figure 5 compares the target and simulated cross-spectral density function and cross-correlation between locations 1 and 2. The match between target and simulated cross-spectra are excellent. Note that the apparently large discrepancy in phase at ~ 0.18 Hz is due only to the phase wrap-around effect from $-\pi$ to π.

Figure 6 shows the three measured pressure records, and their simulations using non-Gaussian multi-variate spectral correction. The statistical comparisons shown in Figure 5 are between measured locations 1 and 2 (target), and simulated locations 1 and 2. The low frequency correlation between all three records can be seen in both figures, along with the distinct non-Gaussian characteristics of the measured and simulated records.

Comparisons of the target and resultant power spectrum and probability density function of each individual location are omitted for brevity, but compare as favorably as shown in the univariate example seen in Figure 2. Indeed the comments regarding the potential for improved accuracy in the last paragraph of the example in Section 3 are appropriate here as well. Further iteration leads to closer matching between target and realization, making accuracy only a function of allowable iteration time.
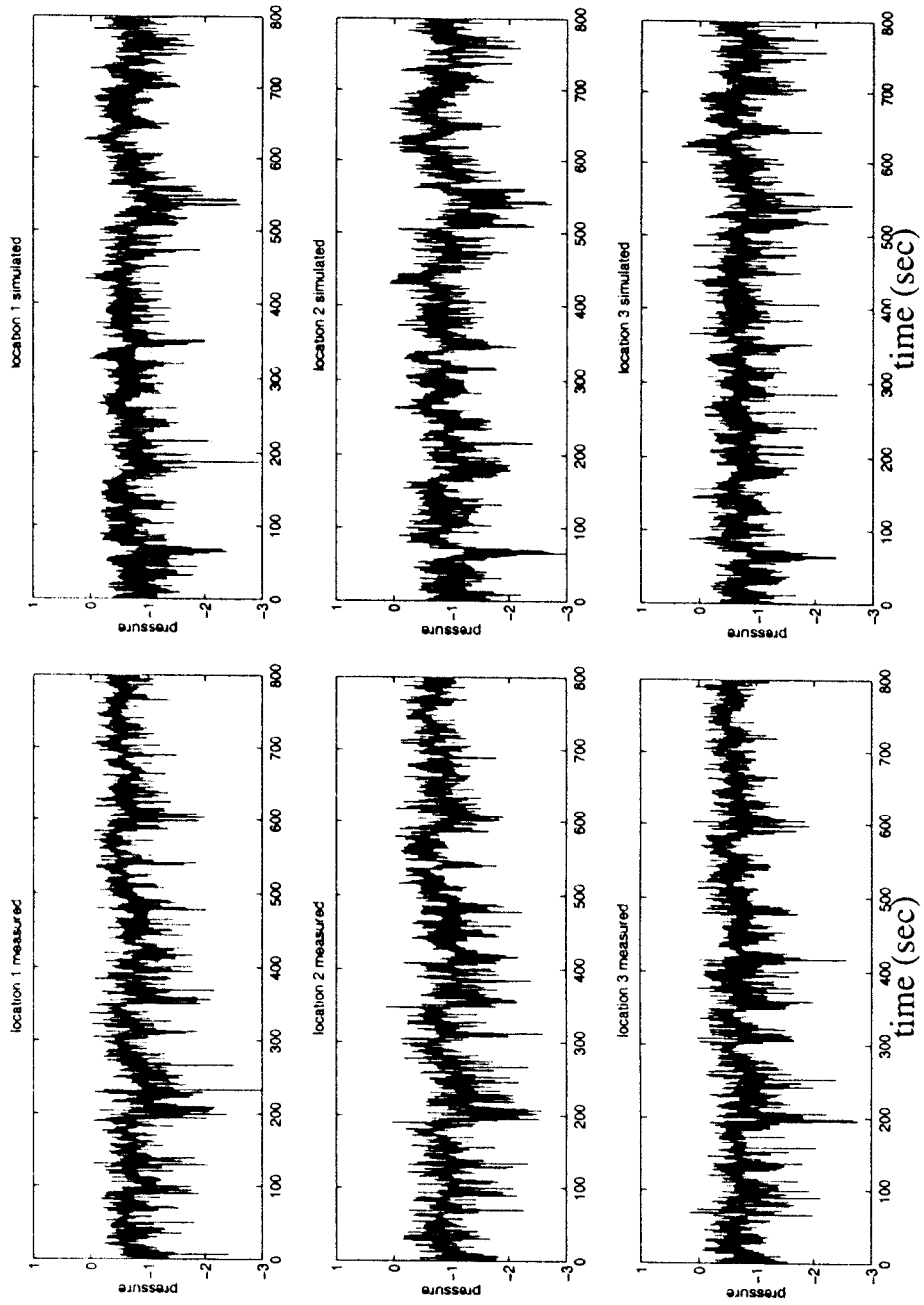
Figure 6.   Left: Measured rooftop pressure at the three locations in Fig. 4. Right: Simulated rooftop pressure at the three locations in Fig. 4.

5. Conclusions

The non-Gaussian uni- and multi-variate spectral correction simulation algorithms are shown to be effective for generating realizations of time histories, at one or more spatial locations, which match target characteristics given in the form of an auto-spectrum, a probability density function, and cross-correlation functions between multiple processes. These algorithms provide additional tools for generating input to Monte Carlo-based simulation methods of structural reliability analysis, particularly for cases where environmental loading differs significantly from Gaussian.

Acknowledgements

References

1. Ammon, D., 'Approximation and generation of gaussian and non-Gaussian stationary processes', *Structural Safety* **8** (1990) 153–160.
2. Elishakoff, I., Ren, Y.J. and Shinozuka, M., 'Conditional simulation of non-Gaussian random fields', *Eng. Struct.* **16**(7) (1994) 558–563.
3. Grigoriu, M., 'Crossing of non-Gaussian translation processes', *J. Eng. Mech., ASCE* **110**(EM4) (1984) 610–620.
4. Grigoriu, M., 'On the spectral representation method in simulation', *Prob. Eng. Mech.* **8** (1993) 75–90.
5. Grigoriu, M., *Applied Non-Gaussian Processes*, PTR Prentice Hall, Englewood Cliffs, NJ, 1995.
6. Gurley, K. and Kareem, A., Analysis, interpretation, modelling and simulation of unsteady wind and pressure data. To appear in the *Journal of Wind Engineering and Industrial Aerodynamics* 1977.
7. Gurley, K., Kareem, A. and Tognarelli, M.A., 'Simulation of a class of non-normal random processes', *International Journal of Nonlinear Mechanics* **31**(5) (1996) 601–617.
8. Lawrence, A.J. and Lewis, P.A.W., 'Modelling and residual analysis of non-linear autoregressive time series in exponential variables', *J. of the Royal Society*, Series B **47**(2) (1985) 162–202.
9. Poirion, F., 'Numerical simulation of homogeneous non-Gaussian random vector fields', *J. Snd. Vib.* **160**(1) (1993) 25–42.
10. Shinozuka, M., 'Simulation of multivariate and multidimensional random processes', *J. of Acoust. Soc. Am.* **49** (1971) 357–368.
11. Shinozuka, M. and Jan, C.M., 'Digital simulation of random processes and its applications', *J. Snd. Vib.* **25**(1) (1972) 111–128.
12. Winterstein, S.R., 'Nonlinear vibration models for extremes and fatigue', *J. Eng. Mech.*, *ASCE* **114**(10) (1988) 1772–1790.
13. Wittig, L.E. and Sinha, A.K., 'Simulation of multicorrelated random processes using the FFT algorithm', *J. Acoust. Soc. Am.* **58**(3) (1975) 630–634.
14. Yamazaki, F. and Shinozuka, M., 'Digital generation of non-Gaussian stochastic fields', *J. Eng. Mech.. ASCE* **114**(7) (1988) 1183–1197.